Journal of Mines, Metals and Fuels, *71(8) : 1045-1057; 2023. DOI: 10.18311/jmmf/2023/35070*

Print ISSN : 0022-2755

Journal of Mines, Metals and Fuels

Contents available at: www.informaticsjournals.com/index.php/jmmf

Opposing and Assisting Flow of a Hybrid Newtonian/ Non-Newtonian Nanofluid Past a Stretching Cylinder

S. Kavya[1,2]* and V. Nagendramma[2]

[1]Narsee Monjee Institute of Management Studies (Deemed to be university), Bangalore - 560083, Karnataka, India; kavya.s@nmims.edu, kavya.s@presidencyuniversity.in

[2]Presidency University, Bangalore- 560064, Karnataka, India; nagendramma@presidencyuniversity.in

Abstract

The prominent perspective of this research is to explore the double solutions for opposing and assisting flows of,

Silver (Ag) – Aluminium Oxide (Al_2O_3) nanoparticles mixture suspended in water (Newtonian)

Silver (Ag) – Aluminium Oxide (Al_2O_3) nanoparticles mixture suspended in blood (non-Newtonian) as its base fluid.

The velocity and temperature jump effects on these hybrid nanofluid flow along with Boussinesq approximation are examined including the impression of effective constraints such as fluid magnetic parameter, curvature parameter and viscous dissipation parameter also with thermal radiation parameter. The reformed set of non-linear governing balances are numerically resolved through the aid of shooting approach associated with Runge-Kutta method of order four. The resulted linear ODEs are then solved using computational MATLAB software. The influence of non-dimensional parameters on flow and thermal profiles are analysed. In additions, variations in friction factor coefficient and values of the amount of heat transmission are deliberated by figures and charts.

Keywords: *Assisting Flow, Boussinesq Approximation, MHD, Opposing Flow, Slip Effects*

1.0 Introduction

Due to the rapid advancement in the engineering and industrial technologies, the most important need in these fields is to intensify the frequency of heat relocation and to escalate the cooling level of the systems in many fields like power generations, nuclear systems, fibre technology, extrusion processes, automobile and electronic applications and many more. To support the concept of cooling, use of hybrid nanofluids is increased[1] first put their idea of nanofluids instead of just fluids. Many models also helped for the improvement in the study of these nanofluids including the models given by[2,3] researchers have studied on different nanofluids and also on hybrid nanofluids[5,6] by observing their influence in heat transfer rate.

The rate of cooling is dissimilar based on the viscosity of the hybrid nanofluids and also on the geometry on which the fluids flow. A cylinder plays a prominent position in rate of heat transfer because of its tremendous applications including preparations of emulsions, refrigerators, thinning copper wires, metal spinning, etc. A model given by[7] explains the fluid flow along a cylinder. Stagnation point flow over a cylinder was explored by[8,9] investigated the solution numerically for the fluid alongside a extending cylinder. The idea by[10] which explained a common boundary condition

**Author for correspondence*

that constitute a fluid jump by the side of the solid liquid crossing point. Many researchers were working on slip effects with distinct fluids in different geometries because of its vast applications including conservation of energy, friction reduction[11,12,13] exposed the mixed convection flows in vertical channels. The work given by[14] presents the stagnation point flow of a mixed convection nanofluid with thermal radiation effect over a stretching or shrinking sheet. Study on MHD mixed convection nanofluid flow past a broadening sheet with slip effects was discovered by.[15] The theoretical solution for a mixed convection flow problem was proposed by[16] worked on boundary layer flow by considering opposing and assisting effects. Mixed convection flow effects of the fluid flow along a horizontal circular cylinder was explained by[17] mixed convection flow problem with constant heat flux and constant wall temperature in a horizontal cylinder was discussed by[18] while[19] explained the same in viscoelastic fluid with constant temperature[20] explained the effects on entropy optimized mixed convection of nanofluid flow along a thin needle with viscosity.[21] Worked on the mixed convection magneto hydrodynamic flow of cross fluid with inconstant thermal conductivity along a non-isothermal surface. Mixed convection of Casson fluid flow along a cone was discussed by.[22] Later[23], studied both assisting and opposing flows of hybrid nanofluid in the direction of a stagnation region of upright plate and investigated[24] on Pseudo plastic nanofluid along a flexible Riga sheet with mixed convection effects. Many works are available on mixed convection flow.[25] Worked on flow of Williamson fluid over a distending cylinder under adjustable thermal conductivity and temperature generation/absorption effects.[26] Investigated on the mathematical solution of MHD Williamson hybrid nanofluid along a stretched cylinder.

The main intent of the existing work is to accord with the influence of velocity jump and temperature slip combinations with variable thermal effects, Boussinesq approximation, dissipation effects of Newtonian/non-Newtonian based hybrid nanofluid under mixed convection effects across a stretching cylinder. No works available on the comparison of Newtonian (water) based hybrid nanofluid together assisting and opposing flow, with non-Newtonian (blood) based hybrid nanofluid in both assisting and opposing flow under velocity and temperature jump effects. The originality of the present study is to give better explanation for the fluctuations in velocity and temperature profiles influenced by distinct prominent parameters with Boussinesq approximation under slip effects of $Ag + Al_2O_3$ + water and $Ag + Al_2O_3$ + blood hybrid nanofluids with the effects of mixed convection (opposing and assisting) flow. The problem is numerically explained using fourth order R-K method and by Shooting technique and the results are plotted with the aid of MATLAB software.

2.0 Mathematical Formulation

The two fold dimensional, steady, incompressible, MHD hybrid nanofluid flow along an expanding cylinder with Boussinesq approximation under velocity jump and thermal slip impacts on the fluid flow influenced with different constraints such as curvature parameter, viscous dissipation parameter and thermal radiation parameter are contemplated in this paper to know the opposing and assisting effects of the hybrid nanofluids flow.

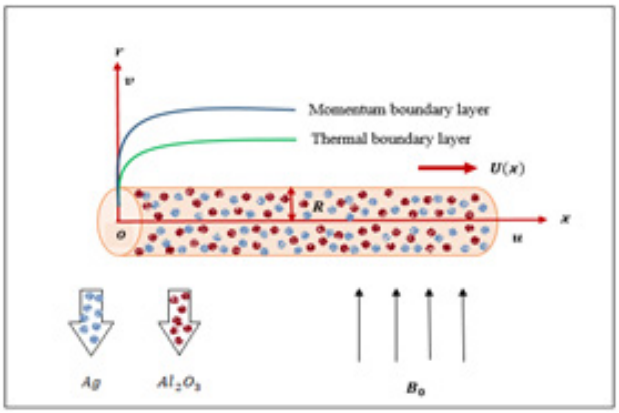

Figure 1. Flow geometry.

Assume the formation of the fluid flow are as given in Figure 1. A coordinate system is formed with -axis over a stretching cylinder and -axis along the normal to the stretching cylinder having reference velocity *U(x)* and with surface temperature T_w *(x)*. For this problem $U(x) = \frac{u_0 x}{l}$ and $\theta(\eta) = \frac{T - T_\infty}{T_w - T_\infty}$. Furthermore, an induced magnetic field strength B_0 is given vertical to the fluid flow. The governing equalities for the above defined model can be formulated as follows[25]:

Conservation of mass:

$$\frac{\partial(rv)}{\partial r}+\frac{\partial(ru)}{\partial x}=0 \tag{1}$$

Conservation of momentum:

$$u\frac{\partial u}{\partial x}+v\frac{\partial u}{\partial r}=\frac{\mu_{hnf}}{\rho_{hnf}}\left\{\frac{\partial u}{r\,\partial r}+\frac{\partial^2 u}{\partial r^2}+\frac{\Gamma}{\sqrt{2}r}\left(\frac{\partial u}{\partial r}\right)^2+\sqrt{2}\Gamma\frac{\partial u}{\partial r}\frac{\partial^2 u}{\partial r^2}\right\}-$$

$$\frac{\sigma_{hnf}}{\rho_{hnf}}{B_0}^2u+\frac{(\rho\beta)_{hnf}}{\rho_{hnf}}g(T-T_\infty) \tag{2}$$

Conservation of energy:

$$u\frac{\partial T}{\partial x}+v\frac{\partial T}{\partial r}=\frac{1}{r}\frac{\partial}{\partial r}\left(r\alpha_{hnf}\frac{\partial T}{\partial r}\right)+\frac{Q(T-T_\infty)}{\left(\rho c_p\right)_{hnf}}-\cdot$$

$$-\frac{1}{\left(\rho C_p\right)_{hnf}}\frac{\partial q_r}{\partial r}+\frac{\mu_{hnf}}{\left(\rho C_p\right)_{hnf}}\left(\frac{\partial u}{\partial r}\right)^2 \tag{3}$$

the boundary conditions are as below:

$$\left.\begin{array}{c} u=U(x)+U_{slip},\qquad v=0, T=T_w+T_{slip}\ at\ r=R,\\ u\to 0, T\to T_\infty\ as\ \ r\to\infty \end{array}\right\} \tag{4}$$

Where, $U_{slip}=\beta_1\frac{\partial u}{\partial r},\quad T_{slip}=\beta_2\frac{\partial T}{\partial r}$ (5)

Table 1. Thermo-physical possessions of mono and hybrid nanofluids

Properties	Nanofluids	Hybrid Nanofluids
Dynamic viscosity	$\mu_{nf}=\frac{\mu_f}{(1-\varphi)^{2.5}}$	$\mu_{hnf}=\frac{\mu_f}{(1-\varphi_1)^{2.5}(1-\varphi_2)^{2.5}}$
Density	$\rho_{nf}=(1-\varphi)\rho_f+\varphi\rho_n$	$\rho_{hnf}=(1-\varphi_2)\left[(1-\varphi_1)\rho_f+\varphi_1\rho_{n1}\right]+\varphi_2\rho_{n2}$
Electrical conductivity	$\sigma_{nf}=\frac{\sigma_n+2\sigma_f-2\varphi(\sigma_f-\sigma_n)}{\sigma_n+2\sigma_f+\varphi(\sigma_f-\sigma_n)}\sigma_f$	$\sigma_{hnf}=\frac{\sigma_{n2}+2\sigma_{nf}-2\varphi_2(\sigma_{nf}-\sigma_{n2})}{\sigma_{n2}+2\sigma_{nf}+\varphi_2(\sigma_{nf}-\sigma_{n2})}\sigma_{nf}$ *where,* $\sigma_{nf}=\frac{\sigma_{n1}+2\sigma_f-2\varphi_1(\sigma_f-\sigma_{n1})}{\sigma_{n1}+2\sigma_f+\varphi_1(\sigma_f-\sigma_{n1})}\sigma_f$
Thermal conductivity	$k_{nf}=\frac{k_n+(n-1)k_f-(n-1)\varphi(k_f-k_n)}{k_n+(n-1)k_f+\varphi(k_f-k_n)}k_f$	$k_{hnf}=\frac{k_{n2}+(n-1)k_{nf}-(n-1)\varphi_2(k_{nf}-k_{n2})}{k_{n2}+(n-1)k_{nf}+\varphi_2(k_{nf}-k_{n2})}k_{nf}$ *where,* $k_{nf}=\frac{k_{n1}+(n-1)k_f-(n-1)\varphi_1(k_f-k_{n1})}{k_{n1}+(n-1)k_f+\varphi_1(k_f-k_{n1})}k_f$
Heat capacity	$(\rho C_p)_{nf}=(1-\varphi)(\rho C_p)_f+\varphi(\rho C_p)_n$	$(\rho C_p)_{hnf}=(1-\varphi_2)\left[(1-\varphi_1)(\rho C_p)_f+\varphi_1(\rho C_p)_{n1}\right]+\varphi_2(\rho C_p)_{n2}$
Coefficient of thermal expansion	$(\rho\beta)_{nf}=(1-\varphi)(\rho\beta)_f+\varphi(\rho\beta)_n$	$(\rho\beta)_{hnf}=(1-\varphi_2)\left[(1-\varphi_1)(\rho\beta)_f+\varphi_1(\rho\beta)_{n1}\right]+\varphi_2(\rho\beta)_{n2}$

Table 2. Numerical computational values of nanoelements and base fluids

Physical Properties	Base Fluid		Hybrid Nanoparticles	
	H_2O	Blood	Ag (φ_1)	Al_2O_3 (φ_2)
C_p (J/Kg K)	4179	3617	235	765
ρ (Kg/m^3)	997.1	1050	10500	3970
k (W/m K)	0.6130	0.52	429	40
σ (S/m)	5.5×10^{-6}	4.3	3.6×10^{7}	35×10^{6}
β(1/K)	21×10^{-5}	0.18×10^{-5}	1.89×10^{-5}	0.85×10^{-5}

Further, the thermo-physical properties are specified in Table 1 and the numerical computational values for silver, aluminium oxide, water and blood can be referred with the aid of Table 2. The comparison values for λ, of this current study result with existed result is given in Table 3.

Using the below non-dimensional resemblance transformations, the PDEs in Equations (1) - (4) are transmuted to a system of non-dimensional ODEs.

$$\eta = \frac{r^2-R^2}{2R}\sqrt{\frac{u_0}{\nu_f l}},\quad \Psi = \sqrt{\frac{u_0\nu_f}{l}}Rxf(\eta),\quad \alpha_f = (\varepsilon\theta+1)\alpha_\infty,$$

$$u = \frac{1}{r}\frac{\partial\Psi}{\partial r} = \frac{u_0 x}{l}f'(\eta),\quad v = -\frac{1}{r}\frac{\partial\Psi}{\partial x} = -\sqrt{\frac{u_0\nu_f}{l}}\frac{R}{r}f(\eta) \tag{6}$$

The Rossel and estimation for thermal radiation is given by,

$$q_r = \frac{-4\sigma^*}{3k^*}\frac{\partial T^4}{\partial r} \tag{7}$$

Where σ* and k* are correspondingly the Stefan-Boltzmann constant besides mean absorption coefficient. By assuming the temperature modification inside the flow, the term T^4 can be revealed as the temperature function. The Taylor series expansion of T^4 about T_∞ is $T^4 = 4TT_\infty^3 - 3T_\infty^4$, after ignoring advanced order relations.

$$\therefore \frac{\partial q_r}{\partial r} = \frac{-16\sigma^* T_\infty^3}{3k^*}\frac{\partial^2 T}{\partial r^2} \tag{8}$$

By switching Equation (6) in Equation (1), undoubtedly it assured the continuity Equation. Moreover, equations (2) and (3) are restored as system of dimensionless ODEs in the following way:

$$(1+2\gamma\eta)f'''(\eta) + 2\lambda f''(\eta) + \lambda(1+2\eta\gamma)^{3/2}f''(\eta)f'''(\eta) + \frac{3}{2}\gamma\lambda(1+2\eta\gamma)^{1/2}[f''(\eta)]^2 + A_1A_2f(\eta)f''(\eta) - A_1A_2\big(f'(\eta)\big)^2 - A_1A_3Mf'(\eta) + A_1A_6\Lambda\theta(\eta) = 0 \tag{9}$$

$$A_4(\varepsilon\theta(\eta)+1)(1+2\eta\gamma)\theta''(\eta) + Rd(1+2\eta\gamma)\theta''(\eta) + \frac{Pr}{A_1}(1+2\eta\gamma)Ec\big(f''(\eta)\big)^2 + A_4\varepsilon(1+2\eta\gamma)\big(\theta'(\eta)\big)^2 + 2A_4\gamma(\varepsilon\theta(\eta)+1)\theta'(\eta) + \gamma Rd\theta' + A_5Prf(\eta)\theta'(\eta) + Pr\beta\theta(\eta) = 0 \tag{10}$$

Where,

$$A_1 = \frac{\mu_f}{\mu_{hnf}},\ A_2 = \frac{\rho_{hnf}}{\rho_f},\ A_3 = \frac{\sigma_{hnf}}{\sigma_f},\quad A_4 = \frac{k_{hnf}}{k_f},\quad A_5 = \frac{(\rho c_p)_{hnf}}{(\rho c_p)_f},\quad A_6 = \frac{(\rho\beta_p)_{hnf}}{(\rho\beta)_f} \tag{11}$$

The transfigured dimensionless boundary conditions exist as shown below:

$$\left.\begin{gathered} f(0) = 0,\ f'(0) = 1+\delta_1 f''(0),\ \theta(0) = 1+\delta_2\theta'(0) \\ f' \to 0,\ \theta \to 0\ as\ \eta\to\infty \end{gathered}\right\} \tag{12}$$

where the non-dimensional constraints presented in the above equations are, magnetic parameter $M = \frac{\sigma_f}{\rho_f}\frac{{B_0}^2 l}{u_0}$, curvature parameter $\gamma = \frac{1}{R}\sqrt{\frac{\nu_f l}{u_0}}$, Williamson parameter $\lambda = \sqrt{2}\Gamma\sqrt{\frac{u_0}{\nu_f l}}\frac{u_0 x}{l}$, thermal radiation parameter $Rd = \frac{16\sigma^* T_\infty^3}{3k^* k_f}$, viscous dissipation parameter $Ec = \frac{u_o^2 x^2}{l^2(T_w-T_\infty)(C_p)_f}$,

Prandtl number $Pr = \frac{\nu_f}{\alpha_\infty}$, mixed convection parameter $\Lambda = \frac{Gr}{Re^2}$. Additionally, $Gr = \frac{g\beta_f(T_w - T_\infty)x^3}{{\nu_f}^2}$ and $Re = \frac{u_0 x^2}{\nu_f l}$ stand for Grashof number and Reynolds number respectively. Eminently note that $\Lambda<0$ denotes the opposing flow and $\Lambda>0$ represents the assisting flow.

The very important physical quantities are defined as follows:

$$C_f = \frac{2\mu_{hnf}}{\rho_f[U(x)]^2}\left[\frac{\partial u}{\partial r} + \frac{\Gamma}{\sqrt{2}}\left(\frac{\partial u}{\partial r}\right)^2\right]_{r=R},$$

$$Nu = \frac{x}{k_f(T_w - T_\infty)}\left[-k_{hnf}\left(\frac{\partial T}{\partial r}\right) + q_r\right]_{r=R} \quad (13)$$

The non-dimensional form of these quantities are:

$$\sqrt{Re}C_f = \frac{2}{A_1}\left[f''(0) + \frac{\lambda}{2}[f''(0)]^2\right],$$

$$\frac{Nu}{\sqrt{Re}} = -[A_4 + Rd]\theta'(0) \quad (14)$$

3.0 Solution Methodology

The dimensionless system of ODEs along with its boundary conditions [Equations (9), (10) and (12)] are resolved into first order ODEs by the RK method unified with shooting technique.

Thus, Equations (8) and (10) can be expressed as,

$$f'''(\eta) = \frac{-f(3)[2\gamma + A_1A_2f(1)] - \frac{3}{2}\gamma\lambda(1+2\eta\gamma)^{1/2}[f(3)]^2}{(1+2\eta\gamma) + \lambda(1+2\eta\gamma)^{3/2}f(3)} +$$

$$\frac{A_1A_2[f(2)]^2 + A_1A_3Mf(2) - A_1A_6\Lambda f(4)}{(1+2\eta\gamma) + \lambda(1+2\eta\gamma)^{3/2}f(3)} \quad (15)$$

$$\theta''(\eta) = \frac{-\left\{(1+2\eta\gamma)\left[\frac{Pr}{A_1}Ec[f(3)]^2 + A_4\varepsilon[f(5)]^2\right]\right\}}{A_4(\varepsilon f(4)+1)(1+2\eta\gamma) + Rd(1+2\eta\gamma)} -$$

$$\frac{\{f(5)[2A_4\gamma(\varepsilon f(4)+1) + \gamma Rd + A_5Prf(1)] + Pr\beta f(4)\}}{A_4(\varepsilon f(4)+1)(1+2\eta\gamma) + Rd(1+2\eta\gamma)} \quad (16)$$

matter to the linear boundary conditions:

$$\left.\begin{array}{c} f(1) = 0, f(2) = 1 + \delta_1 f(3), f(4) = 1 + \delta_2 f(5)\ at\ \eta = 0 \\ f(2) \to 0, f(4) \to 0\ \ as\ \eta \to \infty \end{array}\right\} \quad (17)$$

by using below substitutions,

$$f(\eta) = f(1), f'(\eta) = f(2), f''(\eta) = f(3),\ \theta(\eta) = f(4),$$

$$\theta'(\eta) = f(5) \quad (18)$$

4.0 Validation and Physical Description

In this exploration, the study on opposing flow and assisting flow of a Newtonian (water)/non-Newtonian (blood) based hybrid nanofluid is analysed. In this context, the perception of the numerical out-turn of the present problem is explicated and dispensed evidently through graphs for distinct properties of the engaged foremost parameters on velocity and temperature distributions including skin friction coefficient and Nusselt number.

Figures 2 and 3 exhibit the influence of M on $f'(\eta)$ and $\theta(\eta)$ respectively, which displays that rise in M values brings down the velocity field but boosts the $\theta(\eta)$ and is because, by raising the values of M increases the Lorentz power; therefore due to the more opposing force, it is difficult for the fluid to flow comfortably, hence responsible for decline in $f'(\eta)$ also to come out from the opposing force the fluid worked additionally which later turned as thermal energy and is given in Figure 3.

Improvements in velocity and temperature distributions are observed in Figures 4 and 5 for larger values of γ. Higher the values of γ lesser the radius of the cylinder, so the area between the fluid and the cylinder

Table 3. Comparison Table

λ	Nadeem *et al.*[25]	Malik *et al.*[26]	Present results
0	1	1.005	1.021
0.1	0.976558	0.9565285	0.973885
0.2	0.939817	0.927877	0.932106
0.3	0.88272	0.887909	0.885417

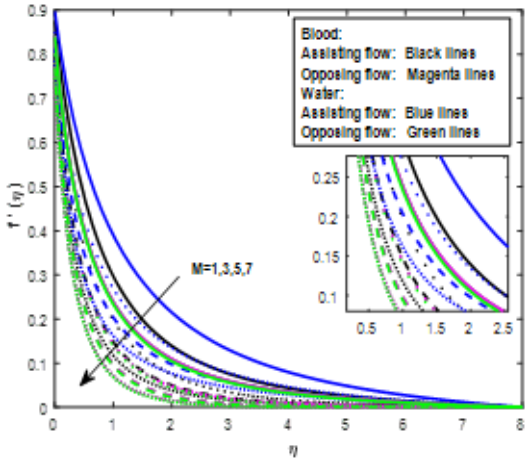

Figure 2. Stimulus of M on $f'(\eta)$.

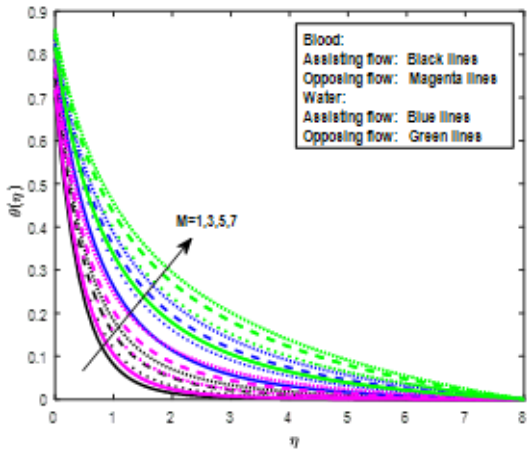

Figure 3. Stimulus of M on $\theta(\eta)$.

diminishes which enhances the fluid velocity. Increasing pattern in $\theta(\eta)$ for accumulative values of γ is due to it increases the average kinetic energy which is accountable for augmented $\theta(\eta)$.

Williamson parameter (λ) effect on $f'(\eta)$ and $\theta(\eta)$ are clearly picturized in Figure 6 and Figure 7 respectively. Higher the values of λ slow down the values of $f'(\eta)$, since increasing entries of λ minimizes the retardation time, which decreases the $f'(\eta)$. Also boundary layer thickness lessens for greater values of λ, so in Figure 7, enhancement in can be observed for inciting λ values.

Figure 8 elucidates the behaviour of ε on the $\theta(\eta)$. $\theta(\eta)$ improves for augmented values of ε, as increase in ε values, the fluid molecules move apart, so the number of electrons increases, which raises the kinetic energy

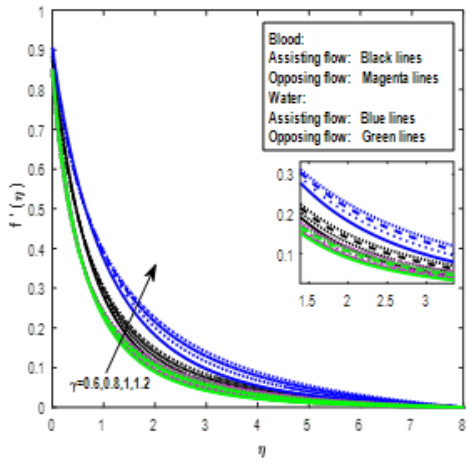

Figure 4. Stimulus of γ on $f'(\eta)$.

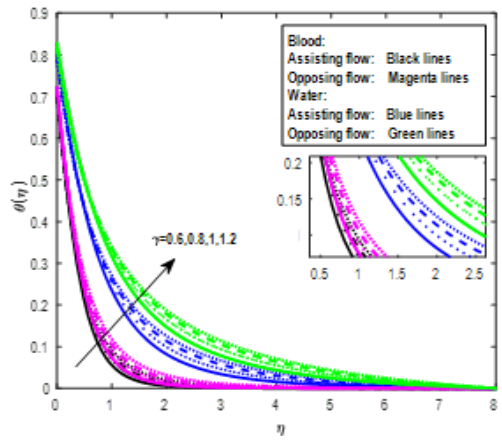

Figure 5. Stimulus of γ on $\theta(\eta)$.

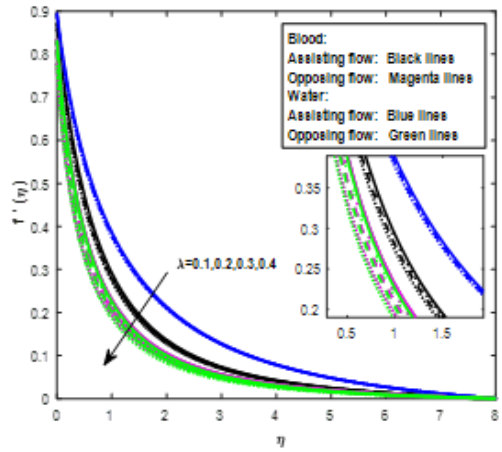

Figure 5. Stimulus of λ on $f'(\eta)$.

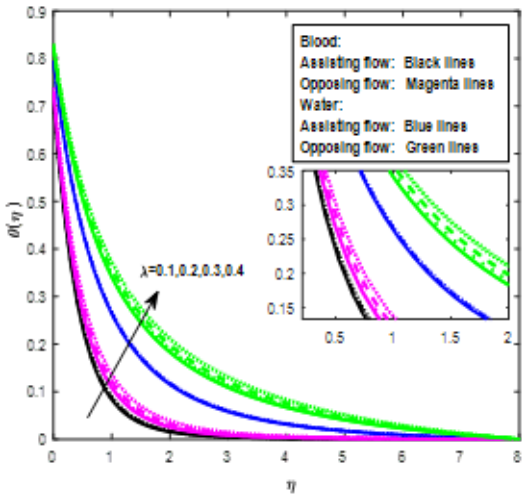

Figure 7. Stimulus of λ on $\theta(\eta)$.

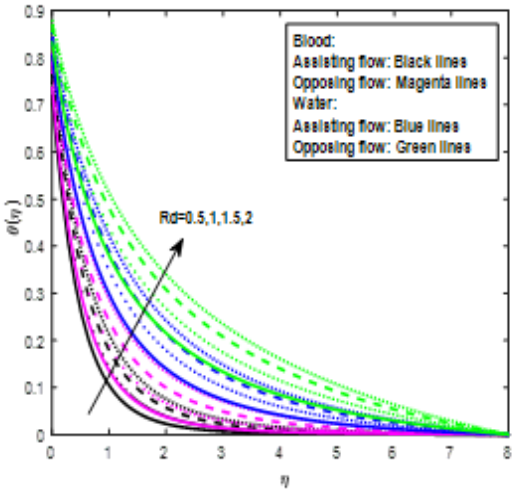

Figure 9. Stimulus of Rd on $\theta(\eta)$.

increases $\theta(\eta)$. Figure 9 is plotted to inspect the nature of temperature field versus *Rd*. The temperature escalates for higher values of Rd. Rising in the values of takes the great responsibility for the discharge of heat from the flow energy of the fluid, hence upturns $\theta(\eta)$.

The impact of β entries on the $\theta(\eta)$ as given in Figure 10. Since during the heat generation process, more heat is produced and increases the $\theta(\eta)$. In Figure 11, the effect in the values of *Ec* on the $\theta(\eta)$. Physically increase in Ec values increases $\theta(\eta)$ due to increase in fluid kinetic energy.

δ_1 Decreases the f'(η) of the fluid which is unambiguously given in Figure 12 and as we increase δ_1, the slip velocity will get incremented so that the velocity of the fluid get decreased. Also, temperature component get increased for upper values of δ_1 and is displayed in Figure 13. The effect on temperature profile due to δ_2 is illustrated in Figure 14, in which we can see that $\theta(\eta)$ decreases for greater values of δ_2. Higher the values of δ_2 lessen the thermal boundary level thickness, wherein some amount of heat is transferred to the fluid from the cylinder, $\theta(\eta)$ reduces.

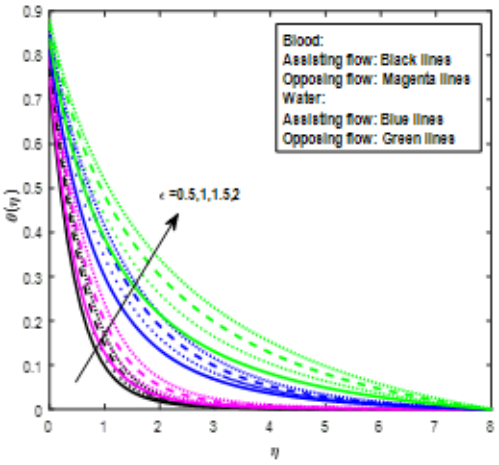

Figure 8. Stimulus of ε on $\theta(\eta)$.

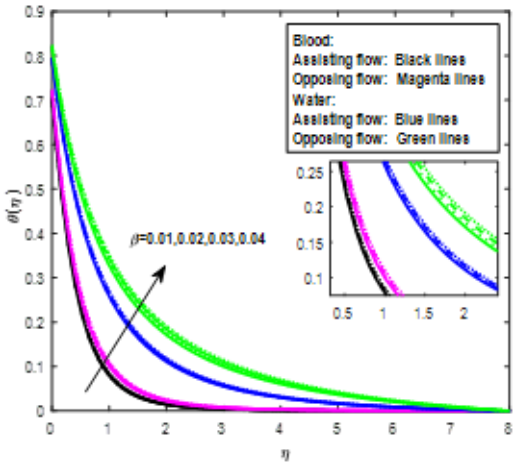

Figure 10. Stimulus of β on $\theta(\eta)$.

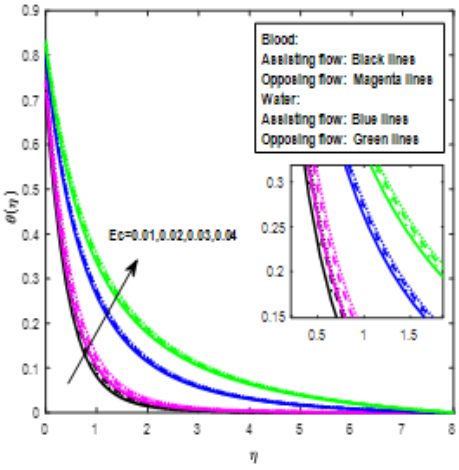

Figure 11. Stimulus of Ec on $\theta(\eta)$.

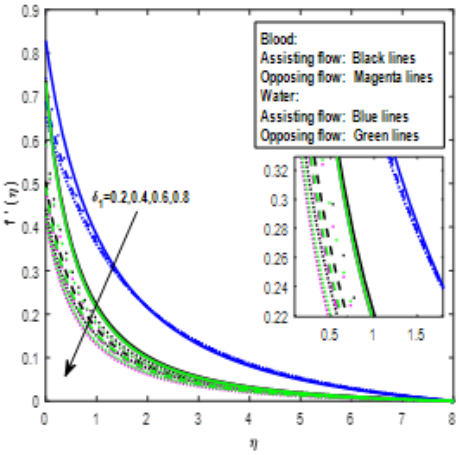

Figure 12. Stimulus of δ_1 on $f'(\eta)$.

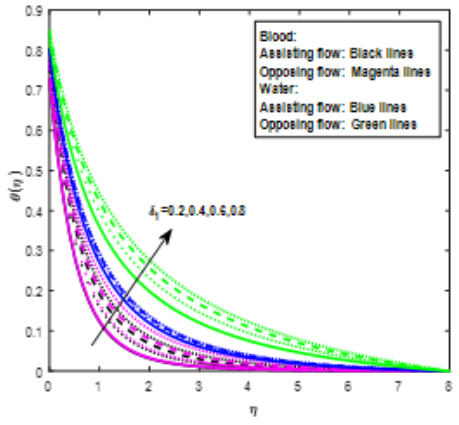

Figure 13. Stimulus of δ_1 on $\theta(\eta)$.

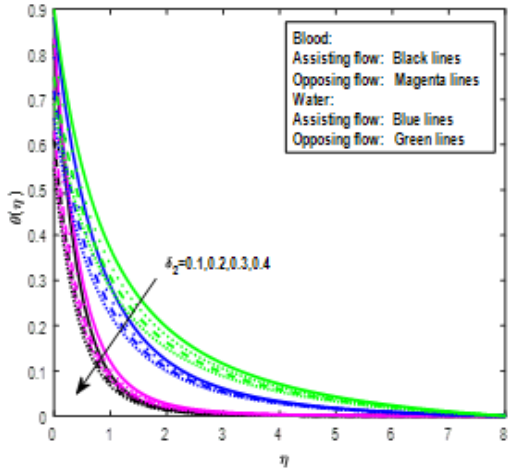

Figure 14. Stimulus of δ_2 on $\theta(\eta)$.

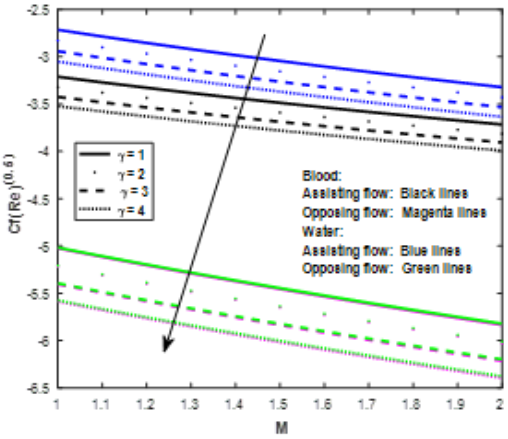

Figure 15. Stimulus of γ, M on $C_f\sqrt{\text{Re}}$.

The effects on $\sqrt{Re}C_f$ for distinct values of γ against M are displayed in Figure 15. Increasing in the values of γ diminishes $\sqrt{Re}C_f$ values γ irrespective of the flow behaviour (assisting or opposing) as well as irrespective of the base fluid (water/blood) for the composed nanoparticles (Ag-Al_2O_3). In addition, in the same figure we can observe that, rise in M also declines skin friction coefficient.

Influence of λ and γ values on $\sqrt{Re}C_f$ is given in Figure 16. We can observe that increase in values of both λ and γ decreases the values of $C_f\sqrt{Re}$. And in Figure 17, augmented in the values of M and γ, declines $\sqrt{Re}C_f$ values.

Effect of δ_1 and M on $C_f\sqrt{Re}$ is elucidated in Figure 18, wherein we can observe that increasing δ_1 values

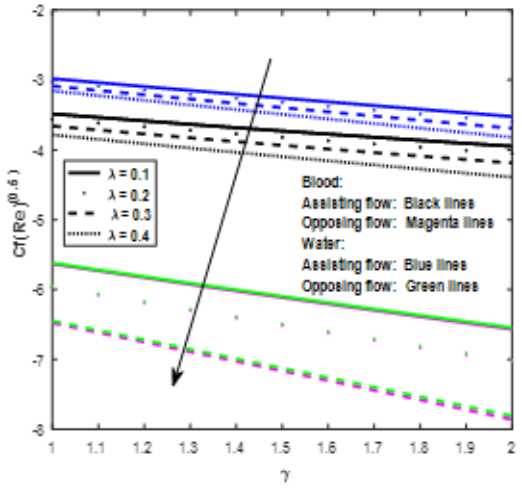

Figure 16. Stimulus of λ,γ on $C_f\sqrt{Re}$.

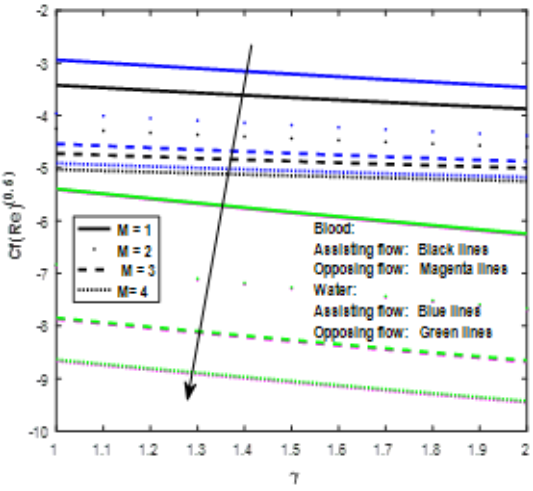

Figure 17. Stimulus of M,γ on $C_f\sqrt{Re}$.

increases $C_f\sqrt{Re}$ as well in the same figure increase in magnetic parameter values declines the values of $C_f\sqrt{Re}$ can be observed. Local Nusselt number increment can be observed for increasing values γ but we can see the decrement in $\frac{Nu}{\sqrt{Re}}$ for raising entries of M can be perceived in Figure 19. Figure 20 is on the influence of λ and γ on $\frac{Nu}{\sqrt{Re}}$, in which more the values of λ decreases the values of $\frac{Nu}{\sqrt{Re}}$ whereas increasing in γ values increases $\frac{Nu}{\sqrt{Re}}$.

In Figure 21, effect of M and γ on $\frac{Nu}{\sqrt{Re}}$ values is given, which shows that increasing values of M diminishes $\frac{Nu}{\sqrt{Re}}$ values, also we can observe, for greater values of γ, the values of $\frac{Nu}{\sqrt{Re}}$ increases as like in Figure 19. Influence of increasing values of ε reduces $\frac{Nu}{\sqrt{Re}}$ values, but raising the

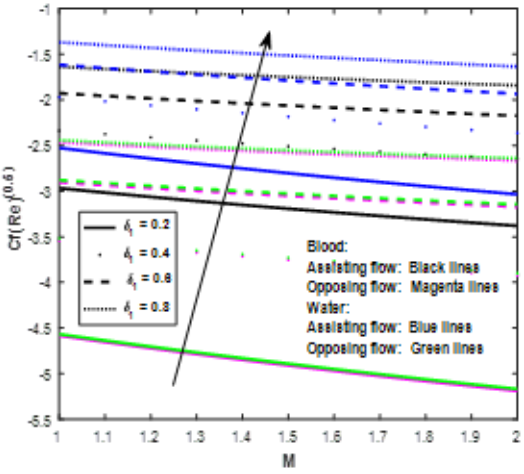

Figure 18. Stimulus of δ_1,M on $C_f\sqrt{Re}$.

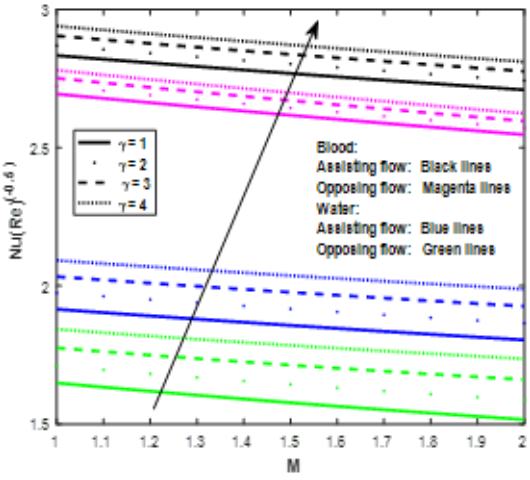

Figure 19. Stimulus of γ,M on $\frac{Nu}{\sqrt{Re}}$.

values of Rd is responsible to increase $\frac{Nu}{\sqrt{Re}}$ values which is clearly given in Figure 22.

$\frac{Nu}{\sqrt{Re}}$ values lessen for the incrementing values of both β and δ_1 which is shown in Figure 23. Increasing Ec values decreases $\frac{Nu}{\sqrt{Re}}$ values as well for increasing M values and is given in Figure 24. Figure 25 explains the effect of δ_1 and on $\frac{Nu}{\sqrt{Re}}$ in which increasing δ_1 and increasing M

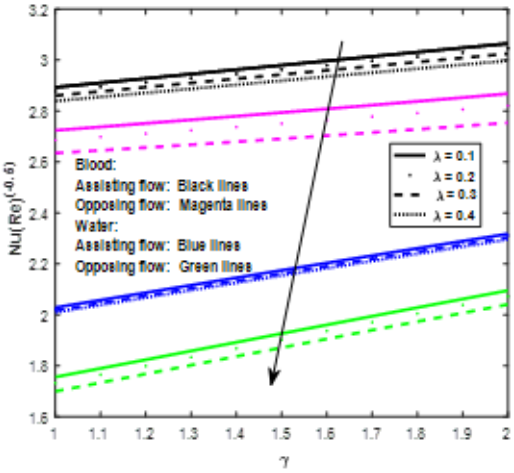

Figure 20. Stimulus of λ,γ on $\frac{Nu}{\sqrt{Re}}$.

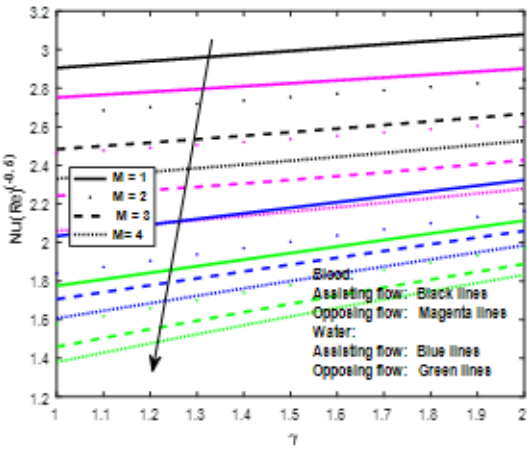

Figure 21. Stimulus of M,γ on $\frac{Nu}{\sqrt{Re}}$.

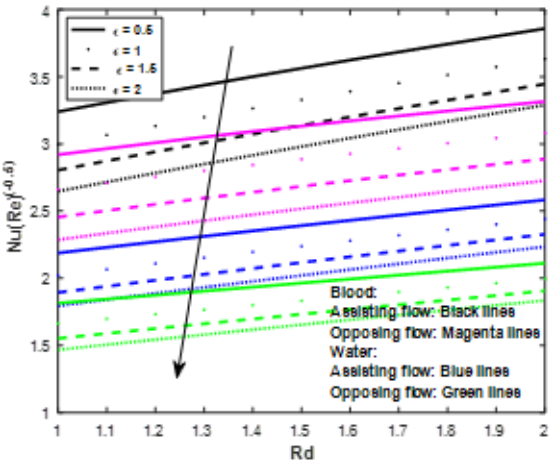

Figure 22. Stimulus of ε,Rd on $\frac{Nu}{\sqrt{Re}}$.

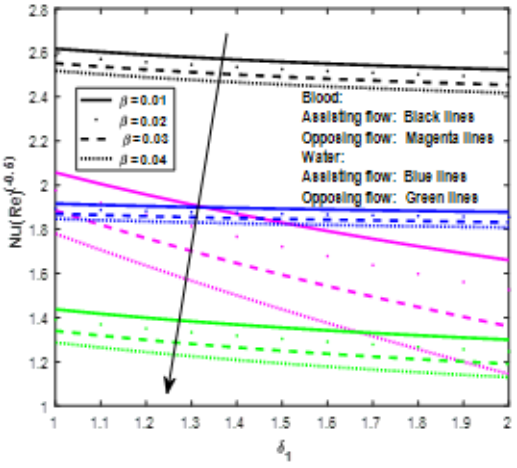

Figure 23. Stimulus of β, δ_1 on $\frac{Nu}{\sqrt{Re}}$.

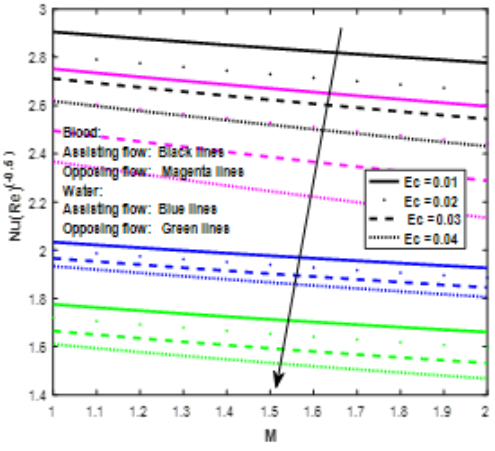

Figure 24. Stimulus of Ec,M on $\frac{Nu}{\sqrt{Re}}$.

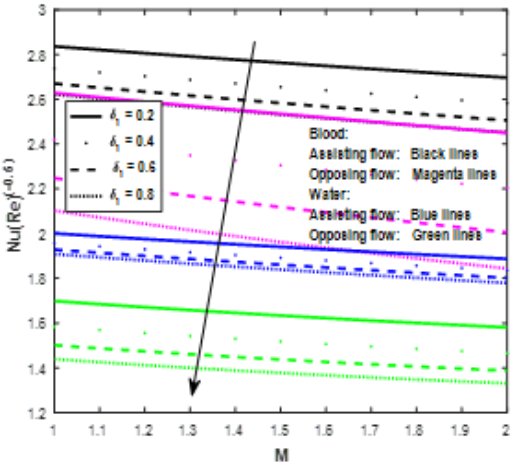

Figure 25. Stimulus of δ_1 ,M on $\frac{Nu}{\sqrt{Re}}$.

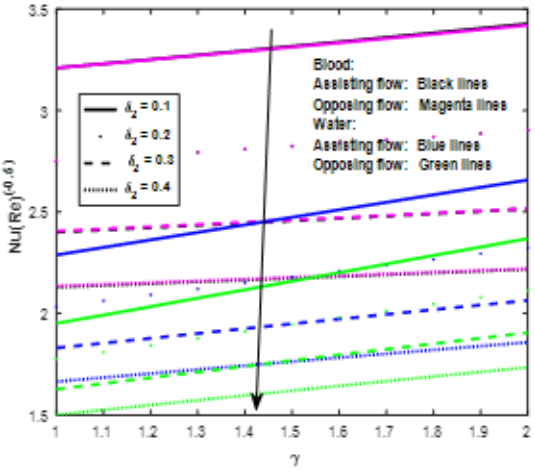

Figure 26. Stimulus of δ_2 ,γ on $\frac{Nu}{\sqrt{Re}}$.

values both diminishes the values of $\frac{Nu}{\sqrt{Re}}$. In Figure 26, decrease in $\frac{Nu}{\sqrt{Re}}$ values can be seen for increasing δ_2 values, but increases for γ values in a considerable manner.

5.0 Concluding Remarks

In this current study, we discussed about the solution for 2D, MHD hybrid nanoparticles mixture (silver-aluminium oxide) in base fluid (either Newtonian - water or non-Newtonian - blood) along a stretching cylinder. The study dealt with the opposing and assisting flow behaviour of the fluid with Boussinesq approximation under velocity and temperature slip effects. A system of ODEs is obtained with the similarity transformation solved from the governing equations. Formerly they are numerically solved via fourth order R-K technique in association with shooting method and by employed with bvp4c MATLAB software to get the solutions for the linear ODEs. The effect of different non-dimensional constraints on velocity component, temperature variation component, skin friction coefficient and Nusselt number are manifested through graphs and tables.

The prominent ouput of the prevailing investigation are as follows:

- The velocity gradient encouraged with the enhancing values of γ, whereas diminished for the larger entries of M,λ and δ_1.
- Greater values of M, γ, λ, ε, Rd, β, Ec and δ_1 result in improvement in temperature distribution except for inciting δ_2 values.
- The skin friction coefficient slumps for higher values of M,λ,γ but raises for the inflation in δ_1 values.
- The Nusselt number lessen by the larger values of M, λ, Ec, ε, δ_1, δ_2 and β, besides it follows an increasing trend for rising values of γ and Rd.
- An increasing pattern on the local coefficient of skin friction can be seen in case of assisting flow than compared with opposing flow.
- Also the considered silver and aluminium oxide nanoparticles mixture suspended in blood has an encouraging impact on the local Nusselt number than the suspension of hybrid mixture in water as base fluid. Hence non-Newtonian (blood) hybrid nanomixture can have more efficient convection than the hybrid mixture suspension in Newtonian (water) base fluid.

6.0 Terminologies

U(x)	Stretching velocity of the cylinder (m/s)
(r,x)	Co-ordinate axes
(u,v)	Velocity components
u_0	Reference velocity (m/s)
R	Radius of the stretching cylinder (m)
l	Specific length (m)
T	Fluid temperature (K)
T_w	Wall temperature (K)
T_∞	Ambient temperature (K)
η	Similarity coordinate
f(η)	Dimensionless stream function
f'(η)	Dimensionless velocity function
θ(η)	Non-dimensional temperature function
Γ	Positive term constant
Ψ	Stream function
B_0	Strength of magnetic field
(ρC_p)	Volumetric heat capacity (J/m^3 K)
μ	Coefficient of viscosity (kg/ms)
k	Thermal conductivity (W/mK)
σ	Electrical conductivity (s/m)
ν	Kinematic viscosity (m^2/s)
ρ	Density of the fluid (kg/m^3)
C_p	Specific heat at constant temperature(J/Kg K)
α	Variable thermal conductivity (Wm^2/J)
M	Magnetic parameter
γ	Curvature parameter
λ	Williamson fluid parameter

Pr	Prandtl number
Ec	Viscous dissipation parameter
β	Heat generation parameter
ε	Thermal conductivity parameter
Rd	Thermal radiation parameter
δ_1	Velocity slip parameter
δ_2	Temperature slip parameter
Λ	Mixed Convection parameter
Λ<0	Opposing flow
Λ>0	Assisting flow
Gr	Grashof number
q_r	Rosseland approximation
σ*	Stefan-Boltzmann constant
k*	Mean absorption coefficient
C_f	Skin friction coefficient
Nu	Nusselt number
Re	Reynolds number
g	Gravity acceleration
$Q(T-T_\infty)$	Heat produce per unit volume
φ	Volume concentration of the nanoparticles
φ_1	Solid volume fraction for Ag
φ_2	Solid volume fraction for Al_2O_3

Subscripts:

f	Base fluid
nf	Nanofluid
hnf	Hybrid Nanofluid
∞	Ambient Condition
n	Nanoparticle
n_1,n_2	First and Second Solid Nanoparticles

7.0 References

1. Choi SUS, Eastman JA, Eastman JA. Enhancing thermal conductivity of fluids with nanoparticles. Developments and Applications of Non-Newtonian Fluids. 1995; 231:99-105.
2. Buongiorno J. Convective transport in nanofluids. ASME J. of Heat Transfer. 2006; 128:240-50.
3. Nield DA, Kuznetsov AV. The onset of convection in a horizontal nanofluid layer of finite depth: a revised model. Int. J. Heat Mass Transf. 2014; 77:915-8.
4. Kuznetsov AV, Nield DA. Natural convective boundary-layer flow of ananofluid past a vertical plate: a revised model. Int J of Ther. Sci. 2014; 77:126-9.
5. Khan WA, Pop I. Boundary -layer flow of a nanofluid past a stretching sheet. International Int J Heat Mass Transf. 2010; 53:2477-83.
6. Khan U, Ahmed N, Khan SIU, Mohyud-din ST. Thermo-diffusion and MHD effects on stagnation point flow towards a stretching sheet in a nanofluid. Propuls. and Power Res. 2014; 3:151-8.
7. Roshko A. Experiments on the flow past a circular cylinder at very high Reynolds number. J Fluid Mech. 1961; 10:345-56.
8. Proudman IAN, Johnson K. Boundary-layer growth near a rear stagnation point. J Fluid Mech. 1962; 12:161-8.
9. Hayat T, Shafiq A, Alsaedi A. MHD axisymetric flowof third grade fluid by a strtching cylinder. Alex Eng J. 2015; 54:205-1
10. Claude - Louis Louis Navier Navier C, Darve C. Memoire sur les lois du mouvement desfuides. Memoires de l'Acdemie Royale des Sciences de l'Institut de France. 2003; 1:389-440.
11. Ellahi R., Hayat T, Mahomed FM. Generalized couette flow of a third-grade fluid with slip: the exact solutions. Z Naturforsch. 2010; 65a:1071-6.
12. Hussain A, Mohyud-Din ST, Cheema TA. Analytical and numerical approaches to squezing flow and heat transfer between two parallel disks with velocity slip and temperature jump. Chin Phys Lett. 2012; 29:114705.
13. Tsang-Yuan Lin. Mixed convection of opposing/assisting flows in vertical channels with discrete asymmetrically heated ribs. J of Thermophys. 1991; 5:415-22.
14. Jamaludin A, Nazar R, Pop I. Mixed convection stagnation-point flow of a nanofluid past a permeable stretching/shrinking sheet in the presenceof thermalradiation and heat source/sink. Energies. 2019; 12:788.
15. Daniel YS, Aziz ZA, Ismail Z, Bahar A, Salah F. Slip role for unsteady MHD mixed convection of nanofluid over strtching sheet with thermal radiation and electric field. Ind J Phys. 2020; 94:195-207.
16. Joshi ND. An analysis of combined free and forcedconvection heat transfer from a horizontal circular cyinder to a transverse flow. J Heat Tranf. 1971; 93:441-8.
17. Sparrow EM. Analysis of mixed convection about a horizontal cylinder. Int J Heat Mass Transf. 1975; 19:229-60.

18. Nazar R, Amin N, Pop I. Mixed convection boundary layer flow past a horizontal cylinder with a constant surface haet flux. Heat Mass Transf. 2004; 40:219-45.
19. Anwar I, Amin N, Pop I. Mixed convection boundary layer flow of a viscoelastic fluid over a horizontal circular cylinder. Int J of Non Linear Mech. 2008; 43:814-35.
20. Shaw S, Patra A, Misra A, Nayak MK. Assisting/opposing/forced convection flow on entropy-optimized MHD nanofluids with variable viscosity: Interfacial layerband share effects. Heat Tranfer. 2022; 1-26.
21. Sultan A, Mustafa M, Rahi M. Assisting or opposing MHD flow of cross fluidalong a non-isothermal surface with variable thermal conductivity. J Mech Eng Sci. 2019; 233(14): 4980-9.
22. Raju CSK, Sandeep N. Opposing and assisting flow characteristics of radiative Casson fluid due to cone in the presence of induced magnetic filed. Int J Adv Sci Technol. 2016; 88:43-62.
23. Waini I, Ishak A, Pop I. Flow towards a stagnation region of a vertical plate in a hybrid nanofluid: assisting and opposing flows. Mathematics. 2021; 9.
24. Aysha Rehman. Assisting and opposing stagnation point Pseudoplastic nano liquid flow towards a flexible riga shhet: a computational approach. Math Probl in Eng. 2021; 14.
25. Nadeem S, Hussain ST, Changhoon Lee. Flow of a Williamson fluid over a stretching sheet. Brazilian J Chem Eng. 2013; 30:619-25.
26. Malik MY, Bibi M, Khan F, Salahuddin T. Numerical solution of Williamson fluid flow past a stretching cylinder and heat transfer with variable thermal conductivity and heat generation/absorption. AIP Advances. 2016; 6:035101.
27. Kavya S, Nagendramma V, Ameer Ahammad N, Sohail Ahmad, Raju CSK, Nehad Ali Shah. Magnetic-hybrid nanoparticles with stretching/shrinking cylinder in a suspension of MoS_4 and copper nanoparticles. Int Commun Heat Mass Transf. 2022; 136:106150.